Supporting Information

Wong et al. 10.1073/pnas.1511830112

SI Materials and Methods

Vector Construction. Full-length synaptotagmin genes were amplified by PCR from the cDNA of rat embryonic day 19 hippocampi using high-fidelity DNA polymerase (Roche) with various appropriate primer pairs (Table S1) and were cut with appropriate restriction enzymes before being ligated into pUS2-GFP to give pSyt1-GFP, pSyt4-GFP, pSyt6-GFP, pSyt7-GFP, pSyt9-GFP, pSyt11-GFP, pSyt12-GFP, and pSyt17-GFP. Protocols of Chung et al. (1) were used to construct the microRNA mimics. DNA fragments containing sequences of complexin or synaptotagmins were cloned into vectors UI4-puro-SIBR or UI4-GFP-SIBR to produce siCpx, siSyt4, siSyt5, siSyt6, siSyt11, and siSyt12. All constructs were verified by restriction enzyme mapping and sequencing. For BDNF-EGFP experiments, we used a Gal4-UAS bipartite system to drive the expression of BDNF-EGFP, as described previously (2, 3).

Cell Culture and Transfection. Low-density cultures of dissociated embryonic hippocampal neurons were prepared as described previously (4). Briefly, hippocampi were removed from embryonic rats (embryonic days 19–20) of a Sprague–Dawley pregnant rat and treated with trypsin for 10 min at 37 °C, followed by gentle trituration. Animal protocols were approved by the Animal Care and Use Committee of University of California, Berkeley. The dissociated cells were plated at a density of 2,500–3,000 cells per square centimeter on poly-L-lysine–coated glass coverslips. The culturing medium was MEM (Invitrogen) supplemented with 5% (vol/vol) FBS (Gemini), MITO$^+$ serum extender (BD Biosciences), Gem21 (Gemini), 20 μM glucose, and glutamax (Invitrogen). After 4 d, the culture medium was changed to Neurobasal (Invitrogen) supplemented with Gem21 and glutamax. We used pyramidal neurons on 12–16 DIV. Cells were transfected on 5–6 DIV using Lipofectamine 2000 (Invitrogen) in Opti-MEM 1 medium (Invitrogen) according to the manufacturer's instructions.

Immunofluorescence Staining. Cells were fixed with 4% (wt/vol) paraformaldehyde and permeabilized with 0.5% Triton X-100. After being blocked with 3% (wt/vol) BSA and 5% (vol/vol) normal goat serum, cells were incubated with primary antibodies overnight at 4 °C. The primary antibodies used were as follows: anti-Syp (clone SY38, Millipore Bioscience Research Reagents), anti- PSD95 (clone 6G6-1C9, Millipore Bioscience Research Reagents), anti–Smi-312 (Covance), anti- MAP2 (Novus), anti-complexin 1/2 (Synaptic System), anti-Syt4 (Synaptic Systems), anti-Syt6 (Neuromab), and anti-EEA1 (Abcam). The preparation was washed with PBS and incubated with secondary antibodies conjugated with Alexa 488, Alexa 555 (Invitrogen), or Cy5 at room temperature. The cells were finally washed with PBS and imaged with wide-field epi-fluorescence microscope (Olympus) equipped with a 60× (NA 1.10 W) water-immersion objective.

Western Blotting. Transfected cells were washed once with PBS and dissolved in radioimmunoprecipitation assay lysis buffer (20 mM Hepes, pH 7.8, 150 mM NaCl, 1 mM EDTA, 0.1% Triton X-100, 50 mM NaF, 1 mM DTT, and protease inhibitor mixture). The cell lysates were cleared by centrifugation at 13,000 × *g* for 10 min, and the supernatants were used for Western blotting analysis. The protein concentration was determined using a BCA kit (Pierce). For Western blotting analysis, equal amounts of cell lysates were subjected to SDS/PAGE and transferred to polyvinylidene difluoride membranes. The membrane was blocked with 5% (wt/vol) skimmed milk and probed with the primary antibody at 4 °C overnight. The primary antibodies used were as follows: anti–c-myc (A-14, Santa Cruz Biotechnology) and anti–β-actin (cell signaling). After the membrane was washed and incubated with HRP-conjugated secondary antibodies at room temperature for 1 h, it was developed with an ECL kit (GE Healthcare).

Preparation of BDNF-QDs. For BDNF-QD imaging, 0.5 μL of 1 μM biotinylated BDNF (5) was incubated with 0.5 μL of 1 μM Qdot655 streptavidin conjugate (Invitrogen) at 4 °C overnight to form the BDNF-QD complex. To separate BDNF-QD complexes from free BDNF-biotin in the mixture, we further purified BDNF-QDs by a Centricon centrifugal filter device (Ultracel YM-100 membrane, Millipore) (Fig. S1, *Left*, right lane). To ensure that BDNF-QDs remain intact after internalization, the TrkB-GFP plasmid was transfected into HEK293T cells, which did not express endogenous TrkB. After 10 nM BDNF-biotin or purified BDNF-QD was applied to transfected cell culture, cell lysates were harvested and subjected to Western blot by anti-biotin, anti-Flag, or anti–β-tubulin antibodies.

To clearly distinguish and trace the individual/single BDNF-QD particle, DIV 12–16 hippocampal neurons were incubated in an extracellular solution with 2% (wt/vol) BSA and various concentrations of BDNF-QDs for 30 min and we then performed time-lapse imaging in the presence of QSY21. The number of endocytosed BDNF-QDs observed in the dendrite or axon increased significantly with increasing BDNF-QD concentration in the range of 0.02–1.6 nM. We detected no significant change in the pattern of QD distribution or movement at different BDNF-QD concentrations. The distance between adjacent BDNF-QDs under 0.2 nM, a concentration that induced a robust neurite elongation in cultured rat hippocampal neurons, averaged 5–10 μm, which could be clearly discriminated (Fig. S2 *B*–*D*). Therefore, we have treated hippocampal neurons with low concentration of BDNF-QD at either 1 nM BDNF-QD for 10 min or 0.2 nM BDNF-QD for 60 min throughout our experiments.

Electrical Stimulation and Time-Lapse Imaging of BDNF-QDs. Coverslips with transfected cells were loaded into a custom-made field stimulation chamber and mounted on the stage of an Olympus upright microscope with a 60× (NA 1.10) water-immersion objective. Cells were perfused at 200 μL/min with a normal extracellular solution: 145 mM NaCl, 3 mM KCl, 3 mM $CaCl_2$, 2 mM $MgCl_2$, 8 mM glucose, and 10 mM Hepes (pH 7.2–7.4) warmed at 30–32 °C using a temperature controller (TC-344B; Warner Instruments). Cells were illuminated with a 300W xenon arc lamp (Lambda LS, Sutter Instruments) with neutral density filter attenuation. Extracellular field stimulation was performed via two parallel platinum wires, yielding fields of 10–15 V/cm. Image acquisition and electrical stimulation were synchronized by Master-8 (A.M.P.I.). TBS comprised 12 trains at 5-s intervals, each train consisting of five 5-Hz bursts of five 2-ms pulses at 100 Hz. The effectiveness of stimulation was assessed by fluorescence Ca^{2+} imaging. Hippocampal neurons were incubated in an extracellular solution containing 2 μM Calcium Orange (Invitrogen) for 30 min and then washed. The filter set for Calcium Orange comprised a 556/20 nm excitation filter, a 595 nm DRLP dichroic mirror, and a 630/95 nm emission filter (Semrock). Time-lapse images were collected at 0.5 Hz with a 14-bit EMCCD camera (iXonEM+ DU897, Andor).

For time-lapse imaging of BDNF-QD, 0.5 μL of 1 μM biotinylated BDNF (5) was incubated with 0.5 μL of 1 μM Qdot655 streptavidin conjugate (Invitrogen) at 4 °C overnight to form the BDNF-QD complex. DIV 12–16 hippocampal neurons were incubated in an extracellular solution with 2% (wt/vol) BSA containing 1 or 0.2 nM BDNF-QD for 10 or 60 min, respectively. Coverslips with BDNF-QD–loaded cells were transferred to a field stimulation chamber in a solution containing 4 μM QSY 21 carboxylic acid, succinimidyl ester (QSY21, Invitrogen). The filter set for observing PSD95-GFP, Syp-GFP, or BDNF-EGFP comprised a 480/17-nm excitation filter, a DA/FI/TR three-band dichroic mirror, and a 525/50-nm emission filter. The filter set for BDNF-QD included a 470/20-nm excitation filter, a DA/FI/TR three-band dichroic mirror, and a 655/15-nm emission filter. The filters were installed in filter wheels and controlled by an optical filter changer (Lambda 10-2, Sutter Instrument). Time-lapse images were acquired (acquisition time, 200 ms) at 0.2 Hz with a 14-bit EMCCD camera controlled by Micro-Manager (6) or NIS-Elements microscope imaging software (Nikon Instruments) during stimulation, delivered as above.

Image and Statistical Analysis. After acquisition, the images were processed for viewing and analyzed with NIH ImageJ software. For the colocalization analyses, images were acquired with identical exposure and gain settings. Channels were thresholded separately to include all recognizable puncta of either GFP fusion protein or the result of immunefluorescent staining. BDNF-QDs were identified as particles. The percentage of colocalization was determined as the percentage of the total number of BDNF-QD particles that overlapped with the thresholded area of the corresponding channel. For the colocalization study of BDNF-QD and BDNF-EGFP, images were analyzed using ImageJ/FIJI plugin Coloc_2 (7). The background fluorescence of BDNF-EGFP was used as a mask to exclude the signal outside the neuron. The Pearson's correlation coefficient was determined as Pearson's *R*-value above the automatic threshold. For the analysis of BDNF-QD release, axon and dendrite segments of interest were selected and linearlized to generate kymographs from time-lapse images. The *y* axis of the kymographs represents recording time, and the *x* axis represents the length (micrometer) of the axonal or dendritic segment images. The time point of BDNF-QD release was determined as the corresponding time to the end point of BDNF-QD trajectory on the kymograph. For the analysis of BDNF-EGFP fluorescence change, a region of interest was circled over the targeted BDNF-EGFP puncta observed on the dendrite of the recorded neuron. To cancel out possible variation of expression levels of BDNF-EGFP and image acquisition conditions among different preparations, we presented data as normalized fluorescence changes ($\Delta F/F_0$), in which fluorescence changes (ΔF) at a given time were divided by the average baseline fluorescence (3 min) before stimulation (F_0). Statistical significance for all quantitation was determined by Student's *t* test, paired *t* test or one-way ANOVA and post hoc analysis. Summary data are given as means ± SEM.

1. Chung KH, et al. (2006) Polycistronic RNA polymerase II expression vectors for RNA interference based on BIC/miR-155. *Nucleic Acids Res* 34(7):e53.
2. Lu H, Park H, Poo MM (2014) Spike-timing-dependent BDNF secretion and synaptic plasticity. *Philos Trans R Soc Lond B Biol Sci* 369(1633):20130132.
3. Matsuda N, et al. (2009) Differential activity-dependent secretion of brain-derived neurotrophic factor from axon and dendrite. *J Neurosci* 29(45):14185–14198.
4. Shen W, et al. (2006) Activity-induced rapid synaptic maturation mediated by presynaptic cdc42 signaling. *Neuron* 50(3):401–414.
5. Xie W, Zhang K, Cui B (2012) Functional characterization and axonal transport of quantum dot labeled BDNF. *Integr Biol (Camb)* 4(8):953–960.
6. Edelstein A, Amodaj N, Hoover K, Vale R, Stuurman N (2010) Computer control of microscopes using μManager. *Curr Protoc Mol Biol*, Chapter 14:Unit14.20.
7. Costes SV, et al. (2004) Automatic and quantitative measurement of protein-protein colocalization in live cells. *Biophys J* 86(6):3993–4003.

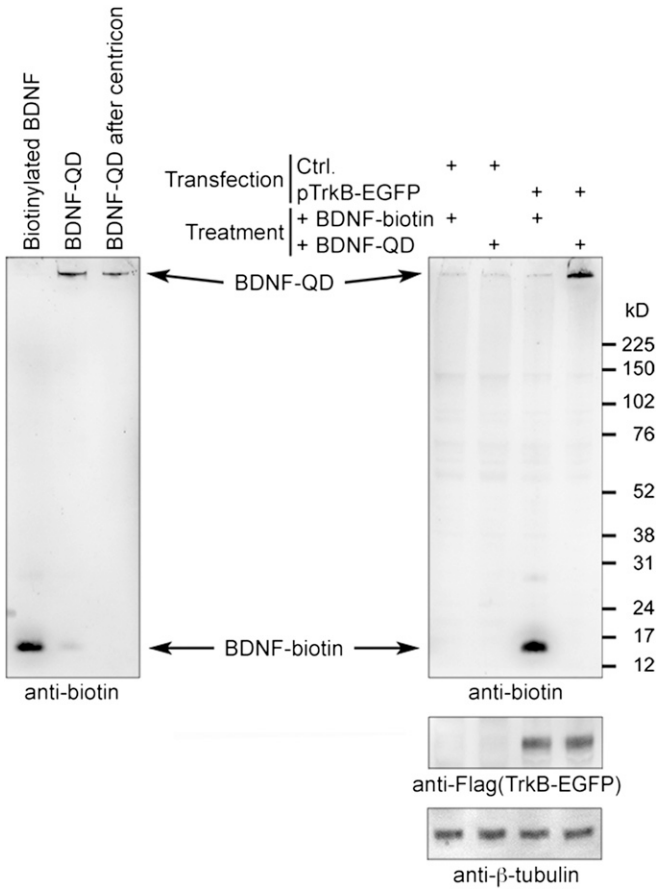

Fig. S1. BDNF-QD remains intact after internalization via endocytosis in HEK293T cells. (*Left*) Biotinylated BDNF (BDNF-biotin, left lane) was incubated with Qdot655 streptavidin conjugate (Invitrogen) at 4 °C overnight to form BDNF-QD complex (center lane). To separate BDNF-QD complexes from free BDNF, the mixture was loaded to a Centricon centrifugal filter devices (Ultracel YM-100 membrane; Millipore) and eluted with 20 mM Hepes buffer (pH 7.2) (right lane). All samples were subjected to Western blot by anti-biotin antibody. (*Right*) HEK293T cells that did not express endogenous TrkB were transfected with a TrkB-GFP plasmid. After 10 nM BDNF-biotin or purified BDNF-QD was applied to transfected cell culture, cell lysates were harvested and subjected to Western blot by antibiotin, anti-Flag, or anti–β-tubulin antibodies. Binding and internalization of BDNF-biotin or BDNF-QD, which remained intact, was specific to the TrkB-GFP transfected cells as shown in the right two lanes. There was no BDNF internalization in the nontransfected cells after 2-h incubation (left two lanes).

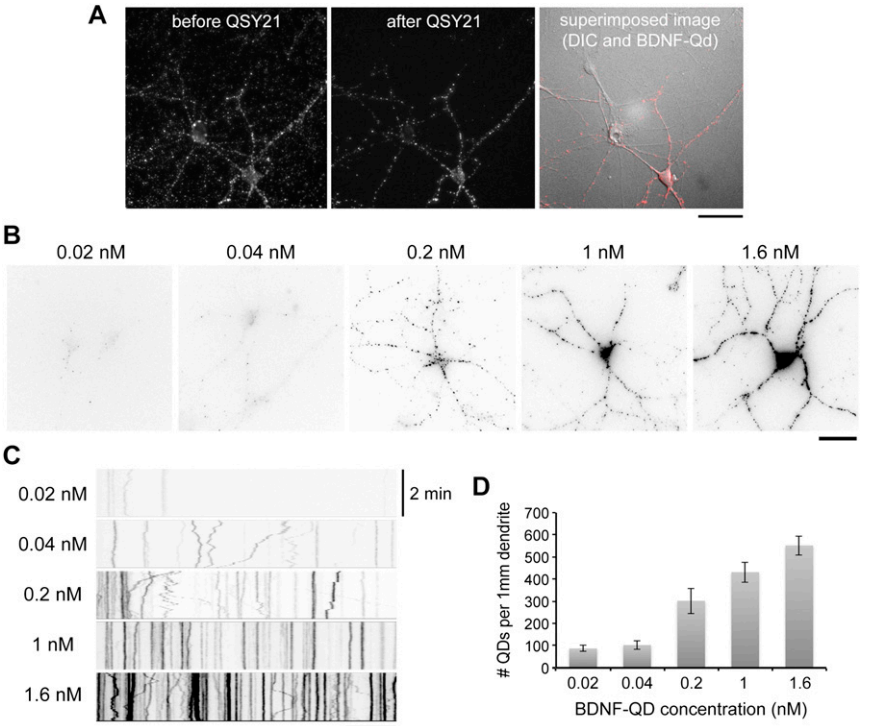

Fig. S2. Internalization of BDNF-QDs at different incubating concentration. (*A*) 1 nM BDNF-QDs were applied to 12 DIV cultured hippocampal neurons for 20 min and then washed out (*Left*). Fluorescence images of live cells were taken before (*Left*) or after (*Center*) QSY21 application. (Scale bar, 50 μm.) (*B*) Typical images showing the number of QD fluorescent dots in a 14 DIV hippocampal neuron increases with BDNF-QD concentration. (Scale bar, 50 μm.) (*C*) Representative kymographs of linearized dendrite segments incubated with various BDNF-QD concentrations. (Scale bar, 10 μm.) (*D*) Average number of BDNF-QDs per 1 mm of dendrites increases with increased BDNF-QD concentration ranging from 0.02 to 1.6 nM ($n = 6$ cells for each concentration; error bar, SEM).

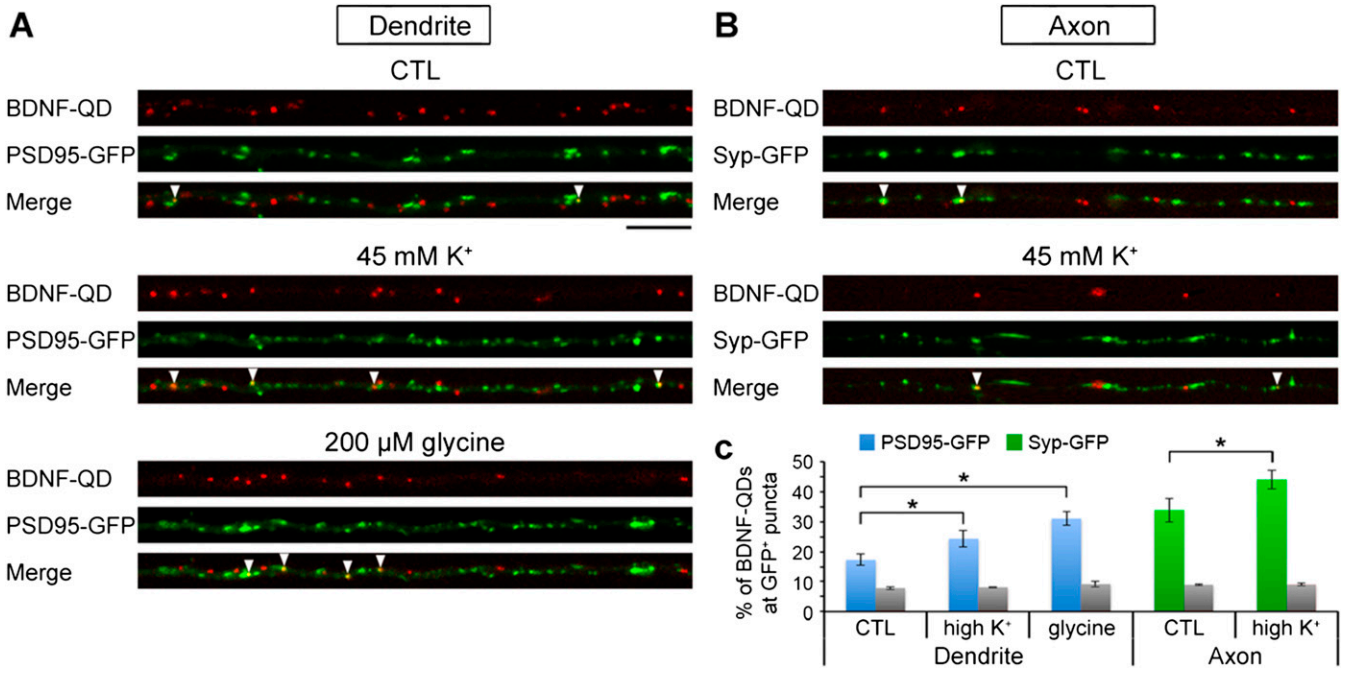

Fig. S3. Activity-induced endocytosis of BDNF-QDs at the axon and dendrites. Dendrites and axons were incubated with BDNF-QDs for 10 min in the presence of 45 mM KCl or 200 μM glycine and then immediately imaged within 10 min. Images showing endocytosed BDNF-QDs along samples of linearlized segments the dendrite (*A*) and axon (*B*) from cultured hippocampal neurons prior-transfected with PSD95-GFP or Syp-GFP and incubated with BDNF-QDs for 10 min in control medium or medium containing 45 mM KCl or 200 μM glycine. Arrowheads: BDNF-QDs colocalized with PSD95-GFP in the dendrite and Syp-GFP in the axon. (Scale bar, 10 μm.) (*C*) Summaries of the percentage of endocytosed BDNF-QDs colocalized with PSD95-GFP and Syp-GFP puncta ($n = 3$–5 independent cultures). Gray bars, percentage of neurite area occupied by PSD95-GFP and Syp-GFP puncta. Error bars, SEM (*$P < 0.05$ by paired t test).

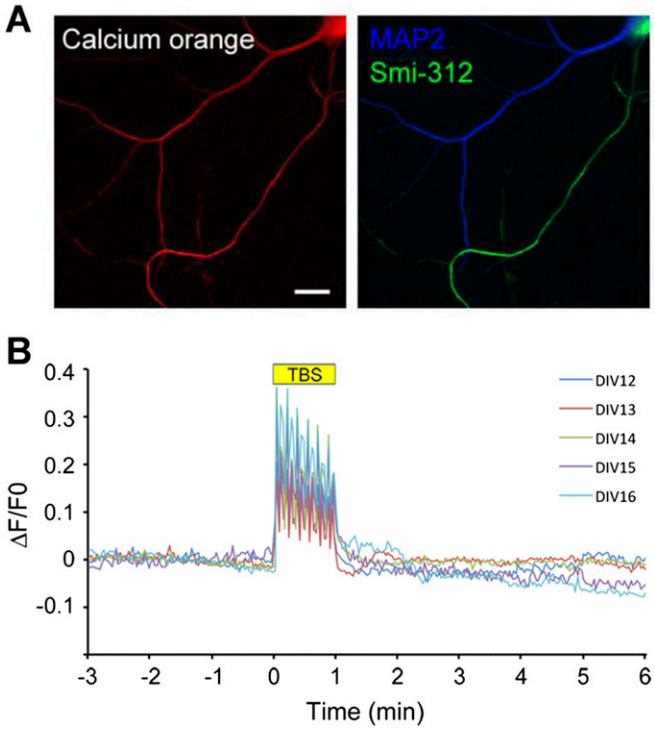

Fig. S4. Stimulation-induced Ca^{2+} elevation at the dendrite. (*A*) Fluorescence image of a live hippocampal neuron loaded with calcium orange (*Left*). The dendrite/axon identity was confirmed by post hoc immunostaining with MPA2 (blue) and Smi-312 (green), respectively (*Right*). (Scale bar, 10 μm.) (*B*) Average changes in Ca^{2+} signals in dendrites of neurons in 12–16 DIV cultures in response to TBS (n = 8–10 neurons for each group).

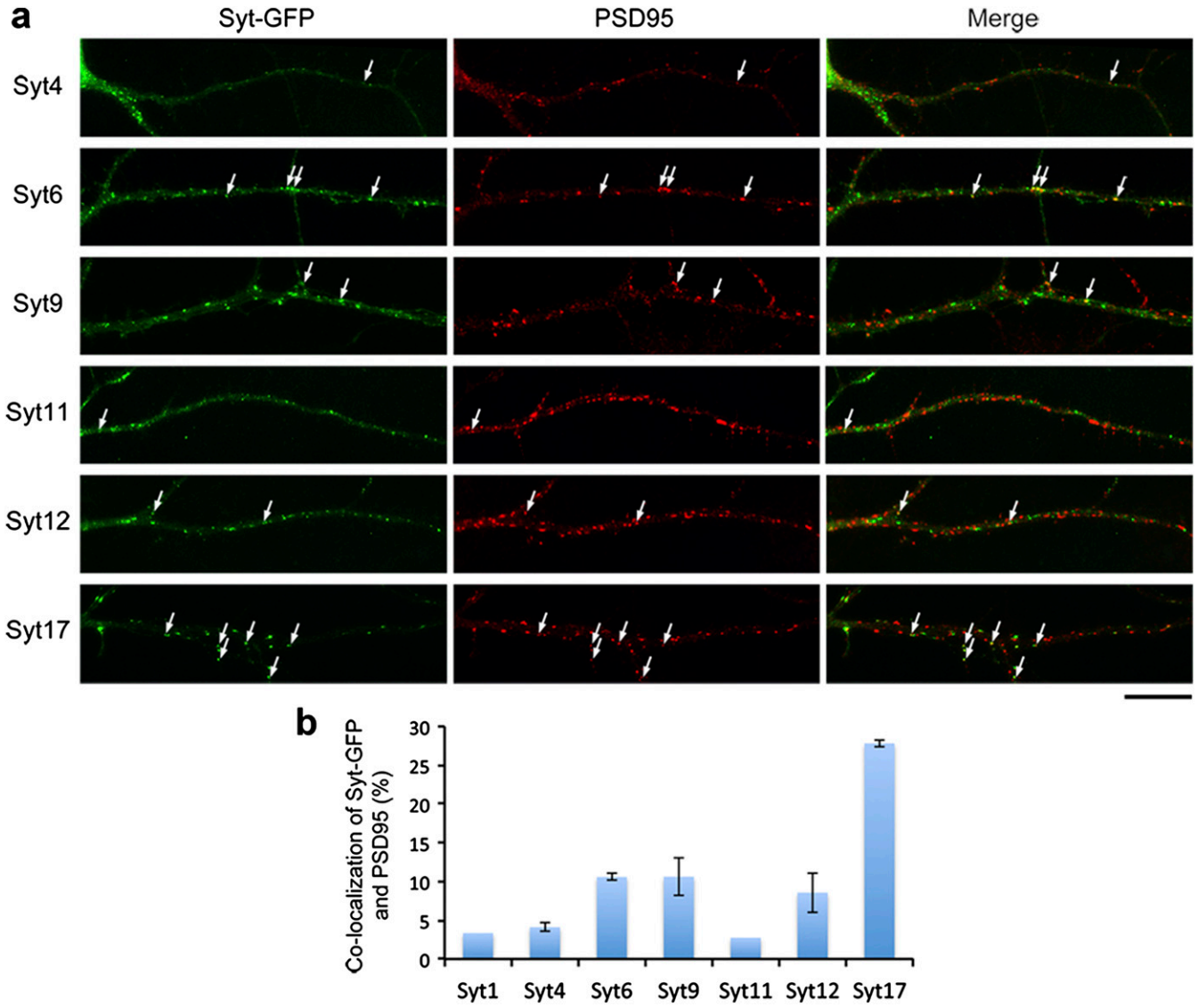

Fig. S5. Synaptic localization of Syt-GFP puncta at postsynaptic sites. (*A*) Example dendrite segments of hippocampal neurons transfected on DIV 6 with one of six different Syt isoforms, each conjugated with GFP, and immunostained for PSD95 (red) on DIV 14. Arrows mark the overlap of Syt-GFP and PSD95 puncta. (Scale bar, 10 μm.) (*B*) Percentage of Syt-GFP puncta that colocalized with PSD95 puncta ($n = 3$–5 neurons each from three to five 12–15 DIV cultures for Syt4, -6, -9, -12, -17; two cultures for Syt1 and -11). Error bars, SEM.

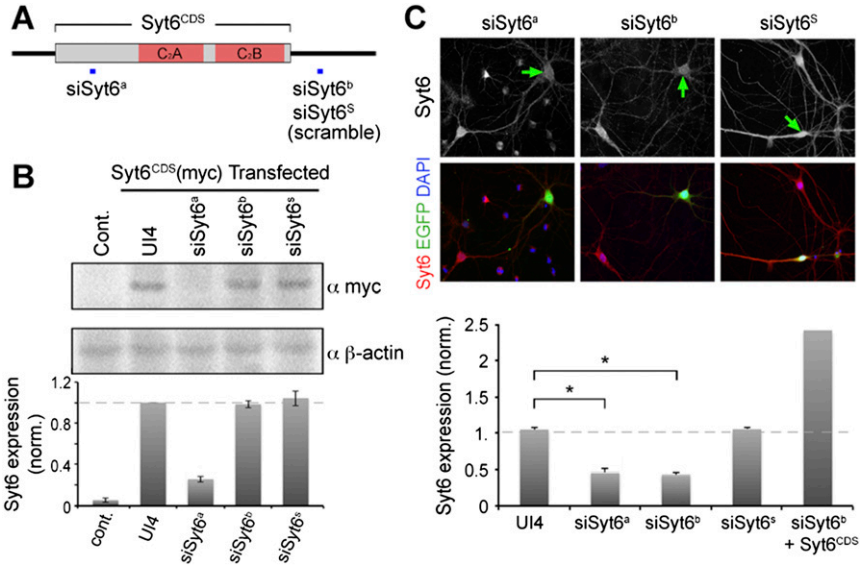

Fig. S6. Western blot verification of the knockdown efficiency of siSyt6 constructs in 293T cells and hippocampal neurons. (*A*) Schematic structure of Syt6, with sites used for generating siRNA constructs (siSyt6^{a}, siSyt6^{b}, and siSyt6^{s} with scramble sequence) marked by a square in blue. (*B*) Western blot analysis of lysates of HEK293T cells transfected with siSyt or backbone vector (UI4) together with Syt6^{CDS}(myc), using anti-myc and anti–β-actin antibodies. Histogram bars below show the density of corresponding immunoblot, with Syt6 expression levels in all blots normalized by that in UI4-transfected cells. Error bars, SEM (n = 3). (*C*) Representative image of hippocampal neurons transfected with siSyt6^{a}, siSyt6^{b}, or siSyt6^{s} (together with EGFP expression) and immunostained for Syt6. Endogenous Syt6 was down-regulated by siSyt6^{a} or siSyt6^{b} efficiently (green arrows, *Left* and *Center*) but not by siSyt6^{s} (green arrow, *Right*). (Scale bar, 10 μm.) Shown below is the quantitation of Syt6 expression levels by measurements of immunostaining intensities, as illustrated in *C*. Relative Syt protein levels were normalized to that of nontransfected neurons in the same image field for all neurons examined. Error bars, SEM (n = 3–6 cells from three 14–15 DIV cultures; *$P < 0.001$ by one-way ANOVA and Tukey post hoc HSD test) (n = 1 culture for the siSyt6^{b} + Syt6^{CDS} group).

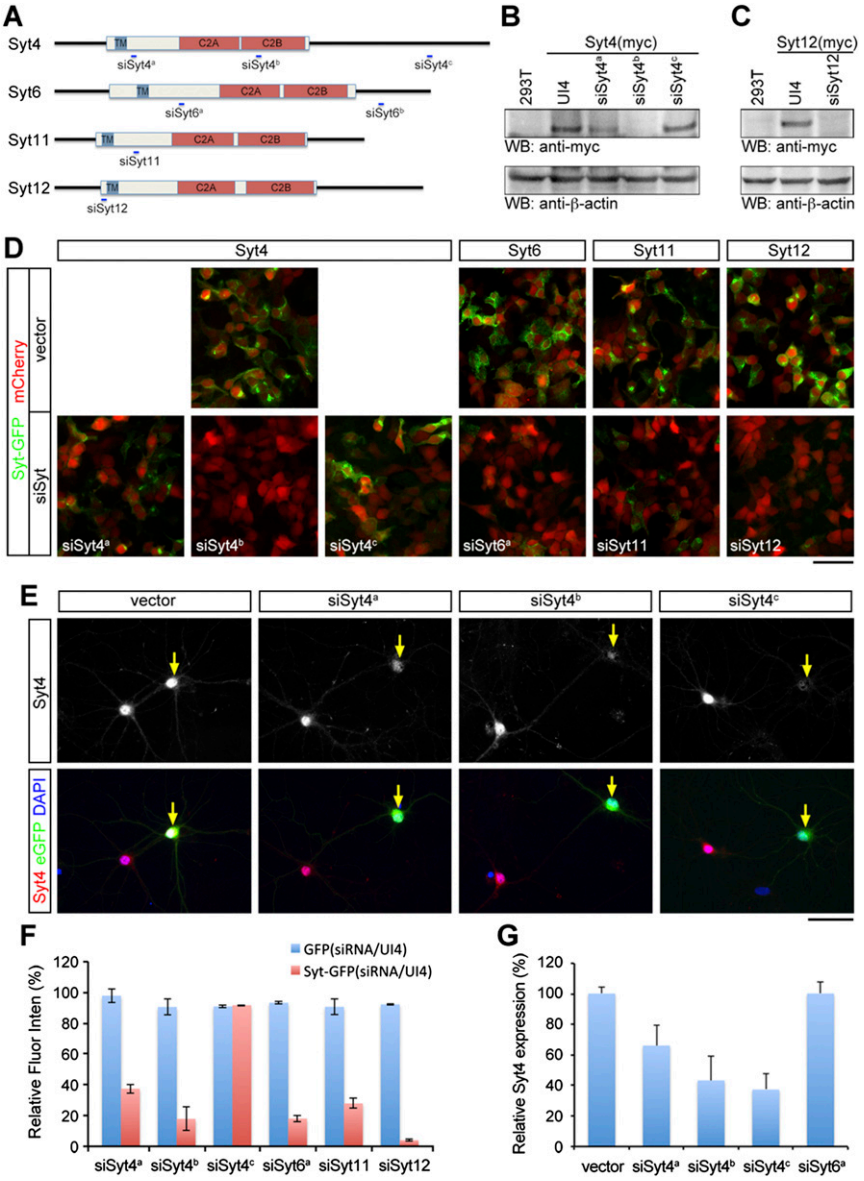

Fig. S7. Western blot verification of the knockdown efficiency of various siSyt constructs against different Syt isoforms in 293T cells and hippocampal neurons. (*A*) Schematic structures of Syt4, Syt6, Syt11, and Syt12. The targeted positions of siRNAs for siSyt4^{a}, siSyt4^{b}, siSyt4^{c}, siSyt6^{a}, siSyt6^{b}, siSyt11, and siSyt12 are marked in bars in blue. (*B* and *C*) Lysates of HEK293T cells transfected with siSyt or backbone vector (UI4) together with Syt4^{CDS}(-myc) or Syt12^{CDS}(-myc) were subjected to Western blotting by anti-myc and anti–β-actin antibodies. (*D*) HEK293T cells were transfected with indicated siSyt constructs or backbone vector together with mCherry and Syt4-GFP, Syt6-GFP, Syt11-GFP, or Syt12-GFP, using mCherry as an internal control for transfection and expression efficiency. Results showed that siSyt4 (siSyt4^{a} and siSyt4^{b}), siSyt6^{a}, siSyt11, and siSyt12 knocked down overexpressed Syt4-GFP, Syt6-GFP, Syt11-GFP, and Syt12-GFP, respectively, in HEK293T cells efficiently. (Scale bar, 50 μm.) (*E*) Hippocampal neurons transfected with siSyt4^{a}, siSyt4^{b}, or siSyt4^{c} (together with eGFP) were immunostained for Syt4. Endogenous Syt4 was down-regulated by siSyt4^{a}, siSyt4^{b}, or siSyt4^{c} (yellow arrows) but not by control vector (*Left*). (Scale bar, 50 μm.) (*F*) Quantitation of results from experiments illustrated in *D*. Relative intensities of GFP or Syt-GFP are first normalized to the mCherry level in the same region of quantitation, and then normalized to the protein amount in cells transfected with UI4 vector. Histograms show average of the GFP or Syt-GFP expression levels. Results showed that siSyt4 (siSyt4^{a} and siSyt4^{b}), siSyt6^{a}, siSyt11, and siSyt12 efficiently down-regulated the overexpressed Syt4-GFP, Syt6-GFP, Syt11-GFP, and Syt12-GFP, respectively, in HEK293T cells, whereas siSyt4^{c}, located in 3′UTR of Syt4, did not down-regulate overexpressed Syt4^{CDS}-GFP. All siSyt plasmids did not affect the overexpressed GFP in these cells, indicating specificity of the siSyt effects. Error bars, SEM. (*G*) Average Syt4 expression level from immunostaining as illustrated in *E*. Relative expression levels of transfected neurons are normalized to the protein level of nontransfected neurons in the same image field. Error bars, SEM.

Table S1. Primers used for plasmid construction

Plasmid	Primers (forward and reverse)
pSyt1-GFP	(F) GCAAGAATTCCAGAACATTTCACTTGAACC
	(R) GCAACTCGAGCTTCTTGACAGCCAGCATGG
pSyt4-GFP	(F) GCAAAAGCTTTCAGCACCTCGGACAGAG
	(R) GCAAGTCGACACCATCACAGAGCATATGCC
pSyt6-GFP	(F) GCAAGAATTCCGCAGCCCTGAGGATCCGG
	(R) GCAACTCGAGCAACCGGGGGGTTCCCTCTT
pSyt7-GFP	(F) GCAAGAATTCATGTACCGGGACCCGGAGGC
	(R) GCAACTCGAGCAGTGGCACCAGCTGAAAGCC
pSyt9-GFP	(F) GCAAGAATTCATGCCCGGGGCCAGGGACGC
	(R) GCAACTCGAGTCGTTTCTCCAGCAGAGAGTG
pSyt11-GFP	(F) GAATTCCAGCCTCTGATTACAACATGG
	(R) CTCGAGGTACTCGCTCAGACTGTGCCAC
pSyt12-GFP	(F) GCAAAAGCTTCACTGCAGGGGACGTCATGG
	(R) GCAACTCGAGGTTTCGCCGGACTGGATGCC
pSyt17-GFP	(F) GAATTCAGATGGCGTACATCCAGTTGG
	(R) CTCGAGGGTCACCTCCAGCGAGGCCGG
siCpx	(F) GCTGTTACTTCTTGAACATGTCCTGCTTTTGGCCTCTGACTGAGCAGGATTGTCAAGAAGTAAC
	(R) TCCTGTTACTTCTTGACAATCCTGCTCAGTCAGAGGCCAAAAGCAGGACATGTTCAAGAAGTAA
siSyt4[a]	(F) GCTGTTAAGCACGTGCACAAACTTGTTTTTGGCCTCTGACTGAATAAGTTGTCACGTGCTTAAC
	(R) TCCTGTTAAGCACGTGACAACTTATTCAGTCAGAGGCCAAAAACAAGTTTGTGCACGTGCTTAA
siSyt4[b]	(F) GCTGTGAAAGTCCAGACACATCAGATTTTTGGCCTCTGACTGAATCTGAGTGTTGGACTTTCAC
	(R) TCCTGTGAAAGTCCAACACTCAGATTCAGTCAGAGGCCAAAAATCTGATGTGTCTGGACTTTCA
siSyt4[c]	(F) GCTGAAGTAGGAGTATCTTAGGCCACTTTTGGCCTCTGACTGAGTGGCCAAGTACTCCTACTTC
	(R) TCCTGAAGTAGGAGTACTTGGCCACTCAGTCAGAGGCCAAAAGTGGCCTAAGATACTCCTACTT
siSyt5	(F) GCTGAGCCCAGCAAGATGGTAGCCAGTTTTGGCCTCTGACTGACTGGCTTCATTTGCTGGGCTC
	(R) TCCTGAGCCCAGCAAATGAAGCCAGTCAGTCAGAGGCCAAAACTGGCTACCATCTTGCTGGGCT
siSyt6[a]	(F) GCTGATAATGTGCTCTTTGACCGACATTTTGGCCTCTGACTGATGTCGGTAAGAGCACATTATC
	(R) TCCTGATAATGTGCTCTTACCGACATCAGTCAGAGGCCAAAATGTCGGTCAAAGAGCACATTAT
siSyt6[b]	(F) GCTGACAAGTGCGGAAATAACATTGCTTTTGGCCTCTGACTGAGTAATGTATTCCGCACTTGTC
	(R) TCCTGACAAGTGCGGAATACATTACTCAGTCAGAGGCCAAAAGCAATGTTATTTCCGCACTTGT
siSyt6[s]	(F) GCTGACATAGTAGGACAAGAGCATTCTTTTGGCCTCTGACTGAGAATGCTTTTCCTACTATGTC
	(R) TCCTGACATAGTAGGAAAAGCATTCTCAGTCAGAGGCCAAAAGAATGCTCTTGTCCTACTATGT
siSyt11	(F) GCTGTATGAGAACCATCTTTGTCCCTTTTTGGCCTCTGACTGAAGGGACAAATGGTTCTCATAC
	(R) TCCTGTATGAGAACCATTTGTCCCTTCAGTCAGAGGCCAAAAAGGGACAAAGATGGTTCTCATA
siSyt12	(F) GCTGAATGATATTCTGTCACGTCCACTTTTGGCCTCTGACTGAGTGGACTGGAGAATATCATTC
	(R) TCCTGAATGATATTCTCCAGTCCACTCAGTCAGAGGCCAAAAGTGGACGTGACAGAATATCATT

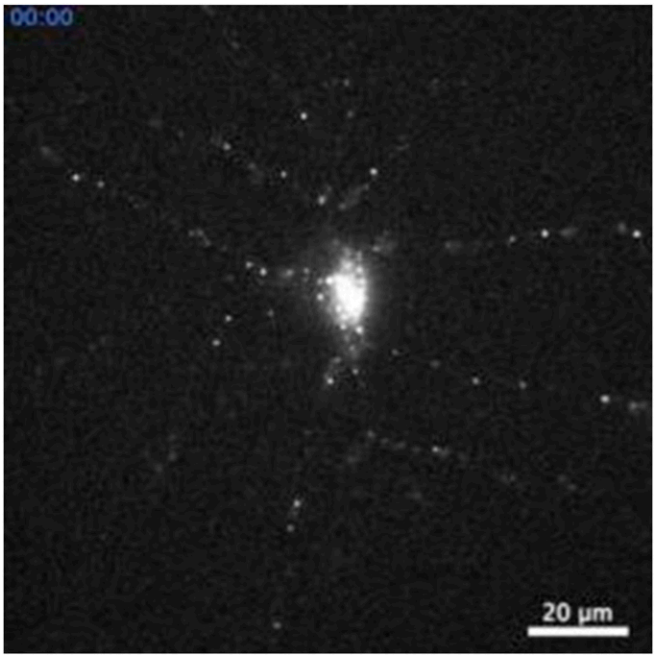

Movie S1. Axonal and dendritic transport of BDNF-QDs. Representative time-lapse images showing the relative motility of BDNF-QDs along the axon or dendrites in 10 DIV hippocampal neurons. Time-lapse sequences of 500 frames were collected at 2-s intervals. The trajectory and kymograph of this video is presented in Fig. 2 *A* and *B*, respectively. (Scale bar, 10 μm.)

Movie S1

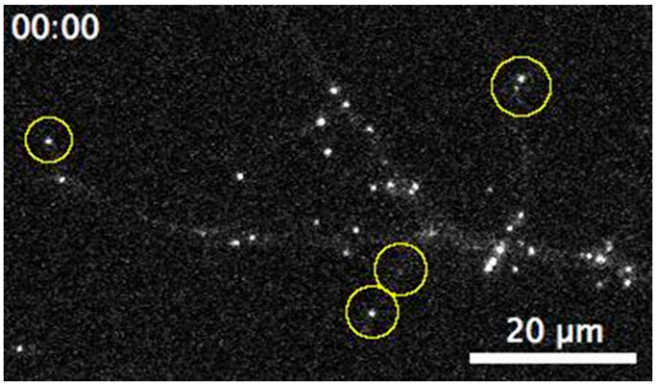

Movie S2. Activity-induced secretion of BDNF-QDs at postsynaptic sites. Time-lapse images of an example neuron containing internalized BDNF-QDs and expressing PSD95-GFP. Time-lapse sequences of 181 frames were collected at 4-s intervals. The kymograph of this video is presented in Fig. 4*C*. The left-bottom yellow-filled circle marks the period of TBS. Yellow open circles mark BDNF-QDs that released upon TBS application. (Scale bar, 20 μm.)

Movie S2

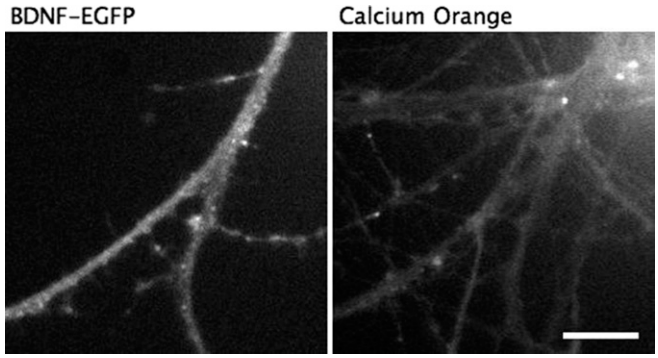

Movie S3. Secretion of BDNF-EGFP upon TBS application. Time-lapse images of an example neuron expressing BDNF-EGFP (*Left*) and stained with calcium orange dye (*Right*). Time-lapse sequences of 200 frames were collected at 5-s intervals. The yellow filled circle marks the period of TBS. (Scale bar, 10 μm.)

Movie S3